Middle East Journal of Applied Sciences
ISSN 2077-4613

Volume : 08 | Issue :01 |Jan.-Mar.| 2018
Pages: 231-250

Hydrochemistry of hot springs and their desalination using membrane distillation in the coastal area, East of Suez Gulf- Egypt

Abo El Fadl, M.M.

Hydrogeochemistry Department, Egyptian Desalination Research Center of Excellence (EDRC), Desert Research Center, El-Matrya, Cairo, B.O.P. 11753, Egypt

Received: 06 Nov. 2017 / Accepted: 14 Feb. 2018 / Publication date: 20 Mar. 2018

ABSTRACT

The structural position of Egypt in the northeastern corner of Africa indicates that it may own significant geothermal resources. These geothermal resources are located along its eastern margin. The most promising areas for geothermal development in Egypt are the northwest Red Sea-gulf of Suez rift system that located along the eastern shore of the Gulf of Suez. It is characterized by superficial thermal manifestations, including a cluster of hot springs with varied temperatures. The specific sites are characterized by high surface temperatures that ranged from 35-45°C at Ayoun Mousa (1, 2) and Hammam Mousa. However, it ranged from 70 - 80°C at Hammam Faroun and Sudr well. The heat for these springs is probably derived from high heat flow and deep circulation controlled by faults associated with rift opening. Complete chemical analyses were achieved for these five samples, where water salinity ranges from 2900 mg/l for Ayoun Mousa1 sample to 15574 mg/l for Hammam Faroun. Direct contact membrane distillation technique was used to desalinate saline samples. Polysulfone membrane was prepared with some modification of nanomaterials such as MWCNTs and SiO_2 meso-porous nanoparticles. The prepared membranes were characterized by scanning electron microscope (SEM), thermal gravimetric analyzer (TGA), contact angle (CA), and FTIR. The flux of polysulfone membrane increased by adding multiwalled carbon nanotubes from 2.2 $l/m^2.h$ for neat polysulfone to 2.5 $l/m^2.h$ at feed temperature 70 °C and permeate temperature 10 °C and feed salinity 20000 mg/l (NaCl). However, at 5000ppm (with the same conditions) , the flux of polysulfone membrane increased by adding multiwalled carbon nanotubes from 2.3 $l/m^2.h$ for neat polysulfone to 5.9 $l/m^2.h$.

Key words: Hot springs, Hydrochemicl species, Water quality, Desalination, Membrane distillation

Introduction

Egypt is bound to the east by what has been interpreted as a median spreading center in the Red Sea and Gulf of Suez. Most thermal springs in Egypt are located along the shores of this Gulf, on the eastern coast at Ayoun Mousa (1, 2), Hammam Faroun, Sudr well and Hammam Mousa Fig. (1). These springs have been known historically since the time of the pharaohs, when they were used for medicinal purposes. Hammam Faroun springs issue from the shore cliff of Gebel Hammam Faroun. The thermal water (70 ^oC) issues from faulted, dolomitic Eocene limestones. The Hammam Mousa spring (known as Moses Baths) is located to the south of Hammam Faroun springs at El- Tor city (Fig. 1), where thermal groundwater issues with a temperature of up to 40^oC from faulted Miocene rocks near the shore. Its waters have been used for bathing since ancient times and are said by many to have the ability to cure skin diseases and arthritis due their high percentage of magnesium, sodium and sulfur (El Ramly, 1969). The Gulf of Suez coastal zones represent the hyper arid province with a cool winter and hot summer. Geothermal energy along the western Gulf of Suez coastal zones are derived from paleo-meteoric water which recharged and flushed residual saline water in the Nubian aquifer under different climatic conditions than the modern ones (El Fiky, 2009). The Gulf of Suez Gulf was formed after the Eocene, as shown by structural trends and sediment distribution of the Cretaceous and lower and middle Eocene. Rifting began in the Gulf of Suez after the Oligocene, and is documented primarily by an Upper Oligocene plantation surface on both sides of the Gulf of Aqaba

Corresponding Author: Abo El Fadl, M.M., Hydrogeochemistry Department, Egyptian Desalination Research Center of Excellence (EDRC), Desert Research Center, El-Matrya, Cairo, B.O.P. 11753, Egypt. E-mail: mmaboelfadl@hotmail.com

and the southern Gulf of Suez (Sturchio *et al.,* 1996). Thermal activity around the Gulf of Suez is controlled by structural elements affecting the entire Gulf region. The hot spring at Hammam Faroun produces sufficient power potential for use at an industrial scale (Lashin, 2007). This spring probably represents deeply circulating groundwater that has ascended to the surface along a fault zone. The value of the estimated geothermal potential for hot springs of East Suez Gulf area was 19.8 MW for an assumed reservoir thickness of 500 m, which would be sufficient for the desalination of water for human and agricultural consumption, and thus useful for sustainable development on the Sinai Peninsula (Abdel Zaher *et al.,* 2011).

In Egypt, desert region constitute more than 94% of the total area of the country. The other 6% of the area includes mainly the cultivated lands in Nile valley and Delta; on the other hand, the majority of Egyptian population is concentrated within the area of the Nile valley and Delta, whereas less than 5% of the population are scattered in all desert areas. The increasing population in Egypt and the limitation of the surface water resources (mainly Nile water) and, accordingly, the limitation of the cultivable lands in the Nile valley and Delta urged the successive governments to draw various programs for land reclamation in desert areas (Salim, 2012 and Said *et al.,* 2013). Desalination is a water treatment process that converts brackish or saline water to fresh water by removing dissolved minerals (e.g. sodium and chloride ions) from the water, and where supplies of brackish or saline water exist, desalination can be used to yield potable fresh water. Most widely applied and commercially proven desalination technologies fall into two categories of thermal (evaporative) and membrane-based methods.

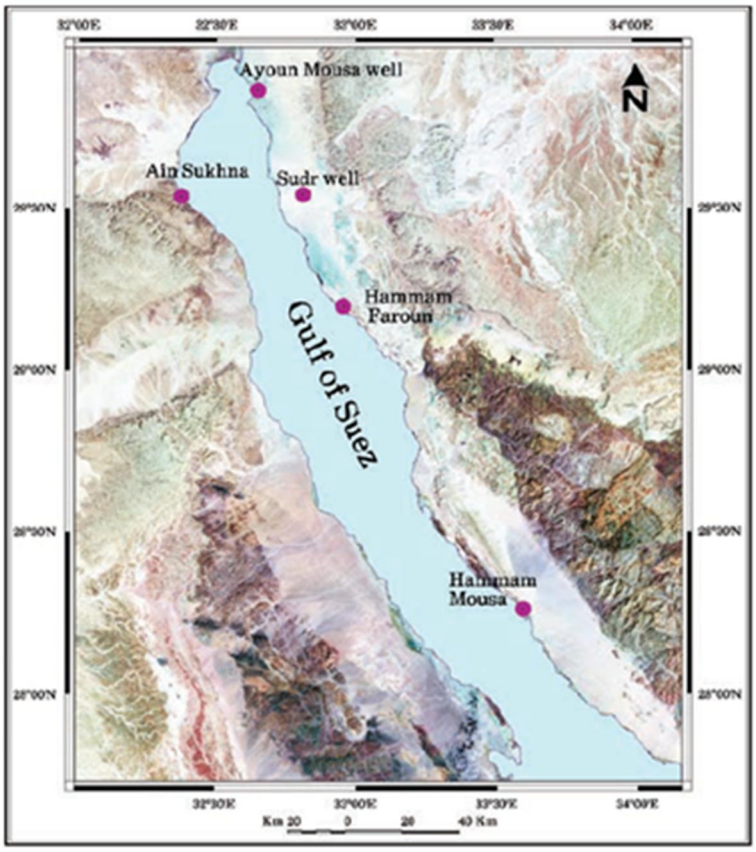

Fig. 1. Location map of the thermal groundwater at the Gulf of Suez region

Advanced desalination membrane processes, which are available now under development to apply by large scale that represent in membrane distillation (MD). It is a thermally driven separation process in which separation is achieved because of phase change. Membrane distillation is a process that applied differences in vapour pressure to permeate water vapour through porous hydrophobic membrane sheet and reject non-volatile component present in the water. Membrane distillation differs from other membrane technologies since the driving force for desalination is not the total pressure of

water through the membrane, but the difference in vapour pressure of water across the membrane as illustrated in fig. (2). In general, the MD driving force may be maintained by one of the four following possibilities applied in the permeate side which were included: i) Direct Contact Membrane Distillation (DCMD) ii) Vacuum Membrane Distillation (VMD) iii) Air Gap Membrane Distillation (AGMD) iv) Sweep Gas Membrane Distillation (SGMD) (Jonsson *et al.,* 1985 and Priya *et al.,* 2014). Direct contact membrane distillation technique in which an aqueous solution colder than the feed solution is maintained in direct contact with the permeate side of the membrane. Both the feed and permeate aqueous solutions are circulated tangentially to the membrane surfaces by means of circulating pumps. In this case, the trans-membrane temperature difference induces the required vapour pressure difference. Consequently, volatile molecules evapourate at the hot liquid/vapour interface, cross the membrane pores in the vapour phase and condense in the cold liquid/vapour interface inside the membrane module.The membranes for membrane distillation are hydrophobic, which allows vapour (but not liquid solution) to pass. The vapour pressure gradient is created by heating the feed solution and cooling/purging the condensate in the permeate side. Therefore, membrane distillation enables separation to occur below the normal boiling point of the feed solution and could utilize low-grade alternative energy.

This study focuses on desalination of hot springs in Suez Gulf area using direct contact membrane distillation technique. The study also focuses on the by preparation and modification of polysulfone membranes with nano-materials. The prepared PSf membrane was characterized using scanning electron microscopy (SEM), thermo-gravimetric analyzer (TGA), contact angle (CA), and FTIR.

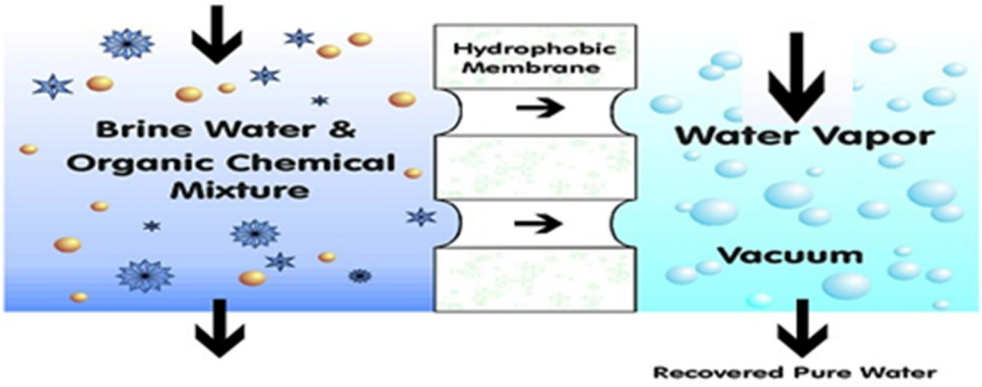

Fig. 2. Membrane Distillation mechanism.

Experimental.

Materials

Polysulfone pellets Udel P-3500 were supplied by Solvay, USA. N, N-dimethylformamide (DMF) was supplied by Fisher Chemical. Multi-wall carbon nanotubes (MWCNTs) product of Arkema Inc was supplied by Aldrich, with Purity >90 % as MWCNTs, the outer diameter (OD) of 10-15 nm& Inner diameter 2-6 nm, lengths: 0.1–10 nm. Silica (SiO_2), meso-porous, 200 nm particle size, pore size 4 nm was supplied by Aldrich. Other reagents such as sodium chloride (NaCl) were of analytical grade and used without further purification.

Water samples and analysis

Field measurements

Field trip to the study sites showed that many active hot springs are located along the Gulf of Suez coastal zones, including Ayoun Mousa (1,2), fig. (3A), Hammam Mousa, fig. (3 B), Sudr well, fig. (3C), and Hammam Faroun, fig. (3D). Most hot springs are located in low-lying beach areas, and are covered with wadi deposits and surrounded by fractured Eocene limestone. The temperature of

thermal water was measured at these sites, and was found to reach 70-80 °C at Hammam Faroun and Sudr well respectively, 35-45 °C at Hammam Mousa and Ayoun Mousa (1, 2).

Fig. 3: The Gulf of Suez coastal zones, including Ayoun Mousa (1, 2) (A), Hammam Mousa (B), Sudr well (C), and Hammam Faroun (D).

Five water samples representing Ayoun Mousa 1 and 2, Sudr well, Hammam Faroun, and Hammam Mousa were collected from the area of study by the author. Temperature, pH, and electric conductivity for samples were measured in the field. The samples collected for cations and anions analysis were stored in polyethylene bottles. All water samples were transported to the laboratory in ice-filled coolers and refrigerated at approximately 4°C until analyzed.

Laboratory analyses

Laboratory analyses for the collected water samples included the measurement of EC, total dissolved salts (TDS), pH, concentration of major ions Ca^{2+},Mg^{2+}, Na^{+}, K^{+}, CO_3^{--} , HCO_3^{-}, SO_4^{--} and Cl^{-}. Measurements were carried out by EC meter model Orion (150 A+), pH meter (Jenway 3510), Flame photometer (Jenway PFP 7), UV/Visible spectrophotometer (Thermo-Spectronic 300). The obtained chemical data are expressed in milligram per liter (mg/l) or part per million (ppm).

Preparation of polysulfone membrane.

Polysulfone casting solution was prepared by dissolving 15 wt. % PSf pellets in DMF at 80–90°C with continuous stirring. The resultant polymer solution was casted on a glass plate with thickness 200 µ using TQC Automatic film applicator and gelled in a water bath. After precipitation, the membranes were washed in de-ionized water, dried completely and kept in dry place until characterization and performance processes.

Modification of Polysulfone membrane using different Nano-particles.

Multi-wall carbon nanotubes (MWCNTs) and meso porous silica (SiO_2) were used to obtain different composite polysulfone membranes. DMF was used as a solvent to assist in the nanoparticles dispersion via sonication technique in order to have good dispersion of nanoparticles in polymer matrix. The composite membrane was prepared by dissolving PSf in DMF as the previous step. For nanoparticles dispersion in polymer solution, a specific weight of nanoparticles was dispersed in certain amount of DMF then adds to the previous mixture (PSf/DMF). The new mixture was vigorously stirred followed by sonication. This solution was later used as a casting solution.

Membrane characterization.

The unused membrane samples used for the chemical and morphological structure analysis were washed with DI water and dried under vacuum before characterization. Membrane morphology was examined by SEM Model Quanta FEG250. The thermal characteristics was carried out by using analyzer TGA-50H, at atmosphere from nitrogen with flow rate 20ml/min and temperature rate holder 10°C/min sample weight varied in rang (1 to 2 mg).Water contact angle (CA_W) was measured using a contact angle instrument (Drop Shape Analyzer-DSA25) with manual components that are fast and simple to operate. De-ionized water was used as the probe liquid in all measurements. Analysis by Fourier transform Infrared spectroscopy was carried out using Broker Vertex70 FT-IR spectrometer.

Performance test.

The module used for membrane performance consisted of two compartments, the feed side and the permeate side. The compartments were made of polyacrylic to resist the corrosion by feed solutions. The module positioned horizontally so that the feed solution flowed through the bottom compartment of the module. While the cooling water passed through the upper compartment. The feed and permeate separated by a membrane with effective area of $0.0018m^2$ fig. (4). The DCMD system was designed by Convergence inspector. The flow rate of feed hot water and permeate cold water were kept constant at 1 L/min. and the temperature of permeate kept at 10 °C where the feed water temperature were varied from 40 to 70°C and the feed water salinity varied from 5000 to 20000 mg/l. All obtained data from the prepared membranes with stable flux, were reported in mean value of the measured flux every hour. The purity of the water extracted was determined through water conductivity using an electrical conductivity meter.

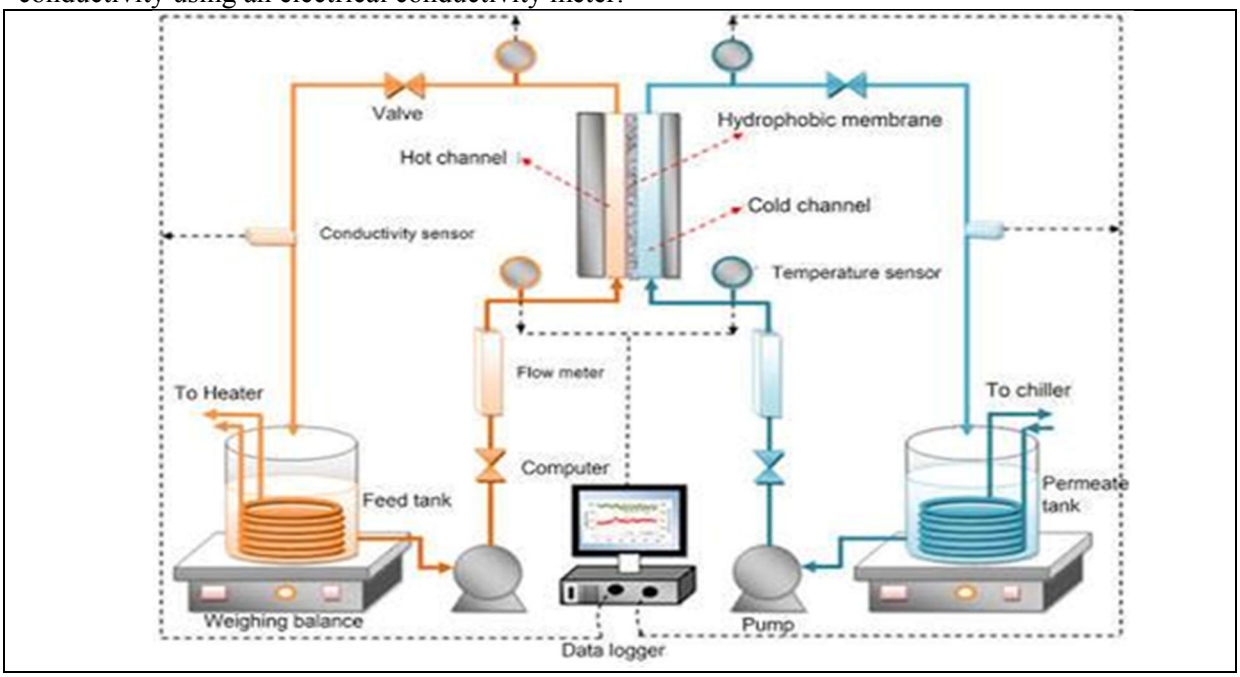

Fig. 4. Schematic Diagram DCMD experimental unit.

Results and Discussion

Hydrogeochemical characteristic of thermal water samples.

Results of chemical analyses of five thermal waters discharged at the Gulf of Suez are given in Table (1). Dissolved ions in the sampled waters in the study area could be mainly derived from reactions of thermal waters with host rocks in addition to mixing of these waters with other water types. Hydrochemical water types were determined using total equivalents of cations and anions. These thermal waters divided into two main groups based on the temperature, table (1). The first group of hot waters (Hammam Mousa, Ayoun Mousa1, 2) having discharge temperatures varying between 35 and 45°C. This group is characterized by water types of Na-Cl. This type may indicate different hydrogeochemical processes such as mixing and water rock interaction.

The second is of hot water reach 70-80 °C at the Hammam Faroun and Sudr well on the eastern coast of the Gulf of Suez. These waters are characterized as Na-Cl type, having total dissolved solids (TDS) value range from 7482 to 15574 mg/l. Concentration of sodium and chloride ranged from 1600 to 4300 and from 3200 to 8774 mg/l, respectively. The high salinity and the Na-Cl water type may reflect that the seawater component of these thermal waters may be high. However, this water type may result from dissolution of Middle Miocene evaporites, which are common in the Gulf of Suez region and reaches a thickness of about 610 m in Ras Lagia in the vicinity of Hammam Faroun (Sturchio *et al.,* 1996).

Table 1: Chemical analysis of major constituents of cations and anions of the thermal water feed and reject MD desalination process at coastal area, East of Suez Gulf-Egypt.

Sample type		pH	EC	TDS	Ca^{++} ppm	Mg^{++}ppm	Na^{+} ppm	K^{+} ppm	CO_3^{--} ppm	HCO_3^{-} ppm	SO_4^{--} ppm	Cl^{-} ppm
Temperature range 35 to 45 °C												
Hammam Mousa	**Feed**	7.4	12500	8813	626.2	378.4	1750	57	0.0	201.9	2800	3100
	Reject	7.6	13330	9462	760	425.3	2100	70	27.6	85.4	1600	4436
Ayoun Mousa 1	**Feed**	7.2	4410	2900	278.2	69.5	680	36	0.0	272.7	550	1150
	Reject	8.1	5510	3532	330	85.1	820	32	27.6	120.8	600	1577
Ayoun Mousa 2	**Feed**	7.5	12760	9864	1100.0	152.4	1950	150	0.0	223.3	3000	3400
	Reject	7.7	13360	10316	1200	160	2200	170	30.0	34.2	2300	4239
Temperature range 70 to 80 °C												
Hammam Faroun	**Feed**	7.6	22480	15574	1017.0	252.8	4300	110	16.8	202.2	1002	**8774**
	Reject	7.8	23000	16980	1150	340.2	4700	120	24	51.2	1300	**9350**
Sudr well	**Feed**	7.4	10660	7482	785.6	155.5	1600	55	0.0	170.8	1600	**3200**
	Reject	7.9	12300	8609	950	218.7	1900	51	6.0	65.9	1300	**4050**

A Piper trilinear diagram (Pipers, 1953) [11], fig.(5) showed that all the thermal water samples, sea water, No, 6 and rain water, No 7 are characterized by the dominance of (Cl^{-}+SO_4^{--}) over HCO_3^{-} and (Na^{+}+K^{+}) over (Ca^{++}+Mg^{++}) except rain water have HCO_3^{-} over (Cl^{-}+SO_4^{--}) and (Ca^{++}+Mg^{++}) over (Na^{+}+K^{+}). Their chemistry probably results from mixing with seawater. Also, it indicated that the thermal water samples showed an increasing trend of Ca and Mg from Hammam Mousa, Hammam Faroun, Ayoun Mousa (2) and sudr well towards Ayoun Mousa (1) which is reflected in the closeness of Hammam Faroun plot to that of the Red Sea. This may indicate that mixing with sea water is possibly high at Hammam Faroun, which is consistent with the high salinity values of thermal water discharged at this locality. However, high salinity values may also be derived from dissolution of thick Miocene evaporites, which can also give rise to the Na-Cl water type.

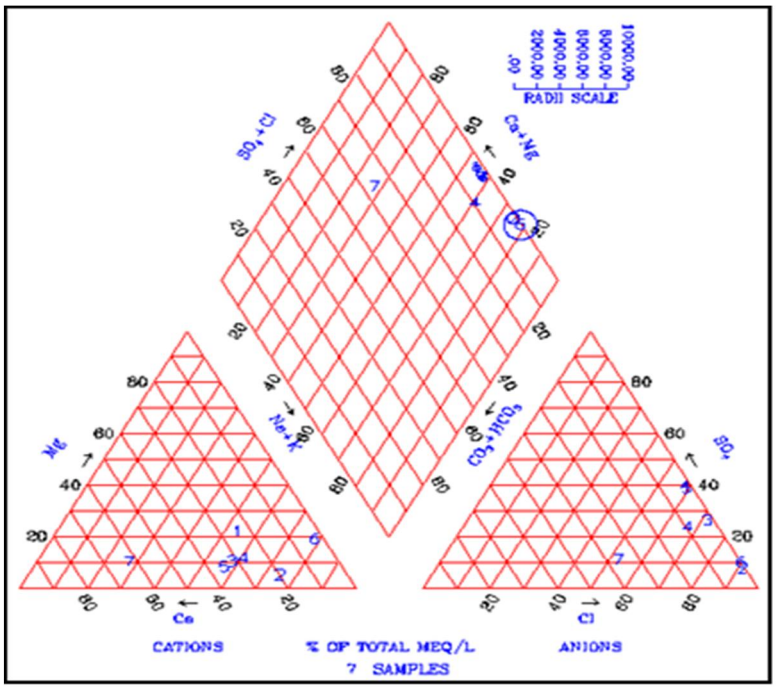

Fig. 5: Piper trilinear diagram for thermal groundwater in coastal east area in Gulf of Suez, Red sea and rain water.

As shown in the Scholler diagram (Schoeller, 1962) fig.(6), thermal waters and rain water have Ca more than Mg. Red seawater give similar signatures as thermal and rain water except for the relative proportions of Ca and Mg, where thermal waters are enriched in Ca. This reflects that mixing with rain water and Red sea water is probably one of the factors responsible for the current hydrochemistry of thermal waters. Due to less Red sea water but more in rain and thermal water, Ayoun Mousa 1 plot at lower levels on the Schoeller diagram. Hammam Faroun thermal waters plot near Red sea water reflecting more mixing with Red sea water. Enrichment of Ca in thermal waters than sea water may be attributed to dissolution of carbonate rocks encountered along the flow path of groundwater, which is enhanced by the increase of temperature

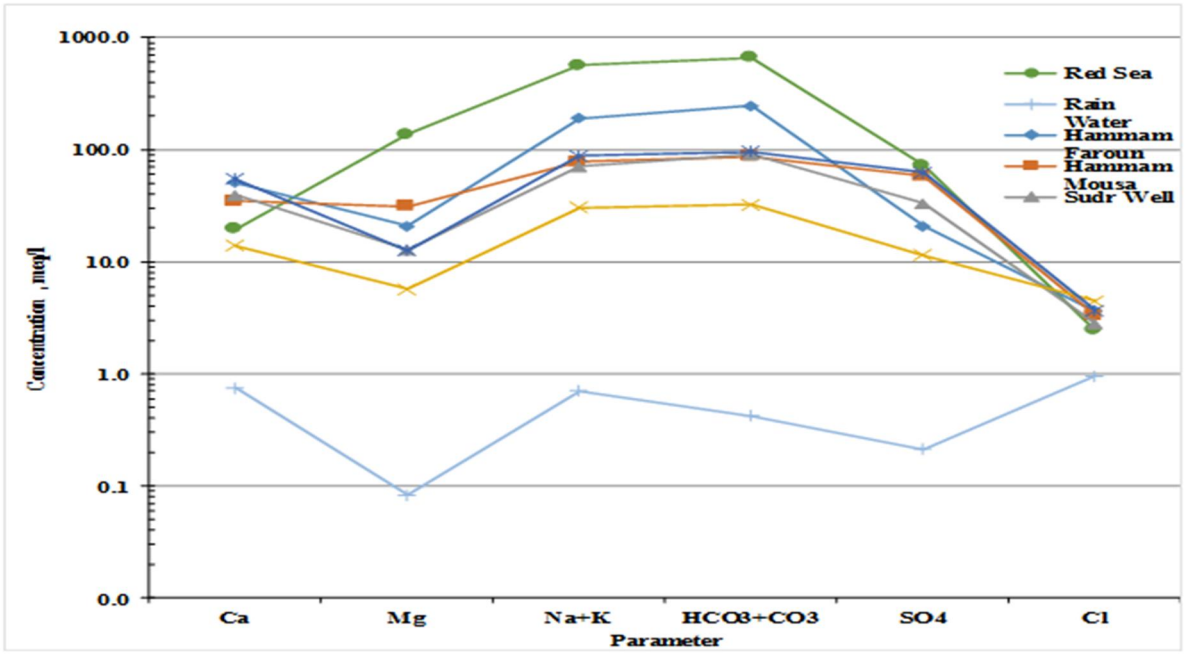

Fig. 6: Scholler diagram for thermal groundwater in coastal east area inGulf of Suez, Red sea and rain water

constituents in thermal water samples from the study area are presented in fig. (7) The high positive correlation between Cl- and Na+ indicates that high Cl- concentrations of thermal water arise from the contribution of sea water or leaching and dissolution of marine rocks.

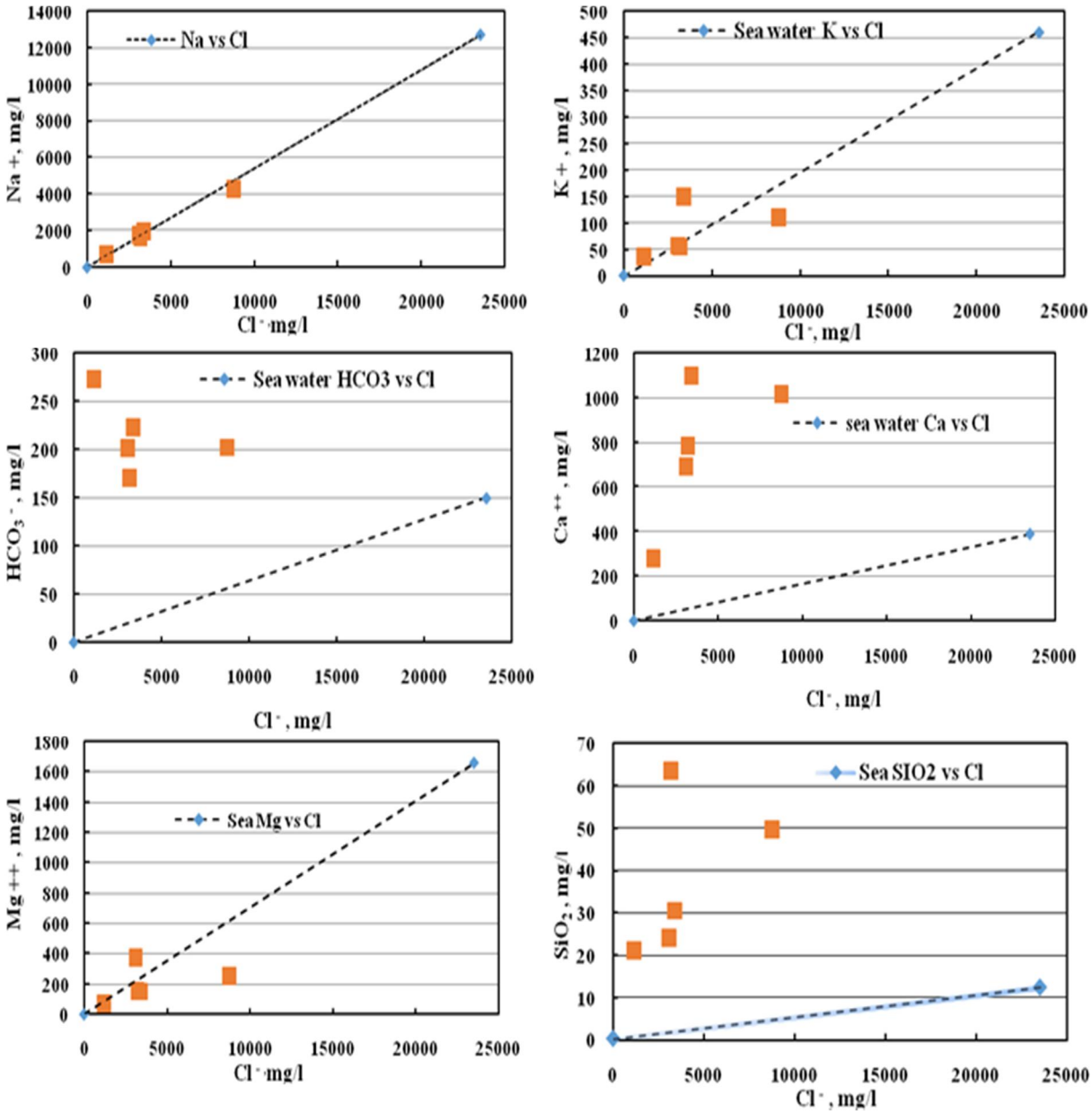

Fig. 7. Correlation coefficients of major and some minor ions thermal groundwater in coastal East Gulf of Suez, Red sea and rain water.

Figure (7) shows that the relations between Na+, K+, Mg++,Ca ++,HCO3-, SiO2 and Cl- strongly confirm the mixing process and contribution of sea water where the plotted points can occur along the mixing line between thermal waters with rain water and sea water. However, thermal groundwater samples are enriched with Ca^{++}, where they are plotted above the mixing line. This can be attributed to the dissolution of carbonate rocks. Thermal water is discharged at Hammam Faroun show high Ca^{++} level, which is possibly derived from faulted, dolomitic Eocene limestones commonly encountered at this locality. According to the relations of the ions fig. (7), it is suggested that the initial aqueous solution was a mixture of sea water and local meteoric water. As the temperature increases, the concentration of SiO_2 is expected to increase, which is observed from the thermal water

samples of the study area. Thermal water samples from Hammam Faroun and Sudr well have the highest discharge temperatures and SiO_2 concentrations. This may indicate that ascending thermal waters at the Hammam Faroun and Sudr well springs is slightly mixed with cold water. Due to this region receives an average amount of rains of about 1000 × 106 m3/y that increase periodically to more than 5000 × 106 m3/y (Shata, 1990). These watershed areas in the Eastern Desert is the main recharge area of groundwater in the Gulf of Suez region. The complex fault systems in this region, which are active in the Quaternary time, play an important role in the recharge and discharge phenomena (Shata, 1990). Such faults allow the formation of discharging conduits for water ascending from depths after being heated and mixed with other water type.

Characterization of prepared membrane

Membrane morphology

The SEM images showed clearly changes in membrane structure, morphology after addition of the nanomaterials, where all membranes exhibit an asymmetric structure fig (8). For the pure PSf membrane, the structure is reasonably consistent spongy structure (Chakrabarty *et al.,* 2008 and Yuxin *et al.,* 2011). In spite of the modified membranes with MWCNTs and SiO_2, the structure showed voids spaces like tubes, tear like and disappear of spongy structure. These void spaces could explain why the mechanical properties of the modified membranes were not as well as the mechanical properties of the pure PSf membrane. Also explained why the modified membrane enhanced MD flux. Furthermore, the surface image showed a slight difference in feature of membranes due to using of nanomaterials, which increase from surface roughness and membrane area.

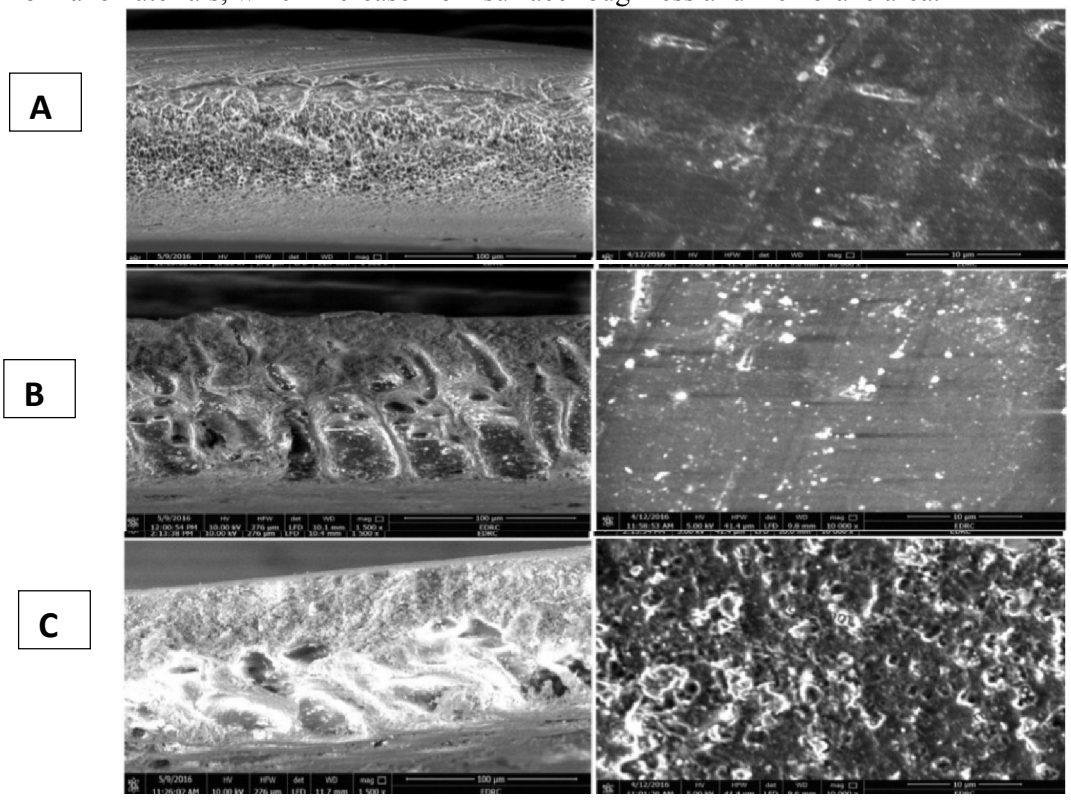

Fig. 8: SEM of surface and cross section for: A) NeatPSf. B) PSf/MW-CNTs. C) PSf/SiO_2

Thermo gravimetric analysis (TGA)

From the analysis of thermo gram curves as shown in fig. (9). At temperature above 500ºC, all membrane showed a greater decrement in weight percentage with the increasing temperature

because they have achieved their decomposition temperature, which take placed on two step first step start in range from (500to 580°C) and second step start from (585to 760 °C). The TGA thermo gram curves showed that the weight losses were in the range of (46.3-63.88 %). The PSF/MWCNTs membrane was the most stable membrane in this range of temperature compared to both unmodified polysulfone membrane and the modified by SiO_2 with its decomposition temperature of 646°C with 46.59% of weight loss. The increment in the degradation temperature can be related to the effect of MWCNTs nano-filler which distinguish with high thermal stability. While Neat PSf membrane showed less decomposition temperature (591°C) and highest weight loss (63.88 %) compared to other membranes. This result accepted with previous work like PSf/TiO_2 and other nano-filler works where improvement of thermal stability by nano-filler addition, (Pourya *et al.,* 2015).

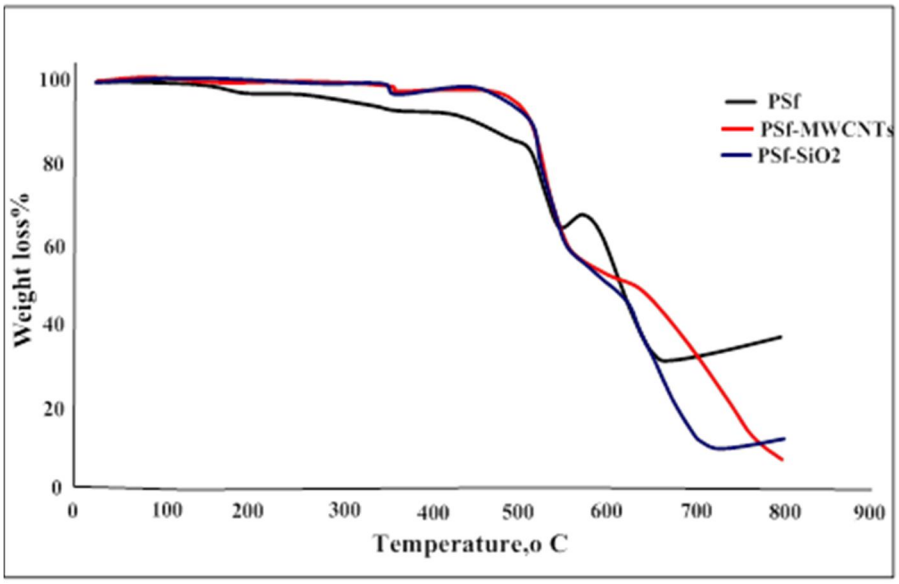

Fig. 9: TGA curves of Neat and modified PSf membranes.

Contact angle measurement:

Hydrophobicity of membrane surface is an important parameter in the MD process. So surface hydrophobicity of nano-composite membrane was studied by determination of the contact angle for neat polysulfone membrane and polysulfone modified with MWCTs and SiO_2 nanoparticles membranes as illustrated in table (2). In case of MWCNTs addition, the hydrophobicity of PSf was enhanced, i.e., increasing the contact angle, this may be attributed to hydrophobic nature of MWCNTs as it do not contain any active functionalized group. These results confirm that the addition of non-functionalized MWCNT increased the hydrophobicity of the composite membrane as reported in the previous work of Okiel *et al.,* (2015); Arsalan *et al.,* 2015 and Madaeni *et al.,* 2013)**.** While, the reduction in the contact angle value with the addition of SiO_2nano-particles may be attributed to oxide forms which form hydrogen bonds with water, so they are more hydrophilic relative to the neat PSf, which means more wetting properties than pure PSf.

Table 2: Contact angle measurements.

PSf conc.Wt. %	Nano-type	Nano-conc.%	Contact angle,°
15	-	-	77
15	MWCNTs	0.5	80
15	SiO_2	0.5	74

Fourier Transform Infrared Spectroscopy (FTIR).

The FT-IR spectra of the neat and the modified PSf membranes were shown in fig. (10). The transmittance bands of the material corresponds to the Polysulfone groups, being in good agreement with standard Polysulfone 1044 cm^{-1} (SO_3H), 1106 cm^{-1} (C-O), 1150 cm^{-1} (R-SO_2-R), 1241cm^{-1} (C-

O), 1488 cm^{-1} (aromatic bond), 2966 cm^{-1} (aliphatic CH), 2879 cm^{-1} (aromatic CH) and 3362 cm^{-1} (OH) which appear in the case of the neat polysulfone membrane which located in the range of hydrogen bond formation. The appearance of broad bands in the range of 450-650 cm^{-1} due to the presence of SiO_2, was absent in this work due to using small concentration of these nano-material (Khare *et al.,* 2002)**.** The intensity of methyl group's pendulum swings near 600 cm^{-1} changes, as well as near 1,550 and 1,639 cm^{-1}. Also shows a change in the interaction nature between the molecular chains, which possibly is realized through their bonds with MWCNTs.

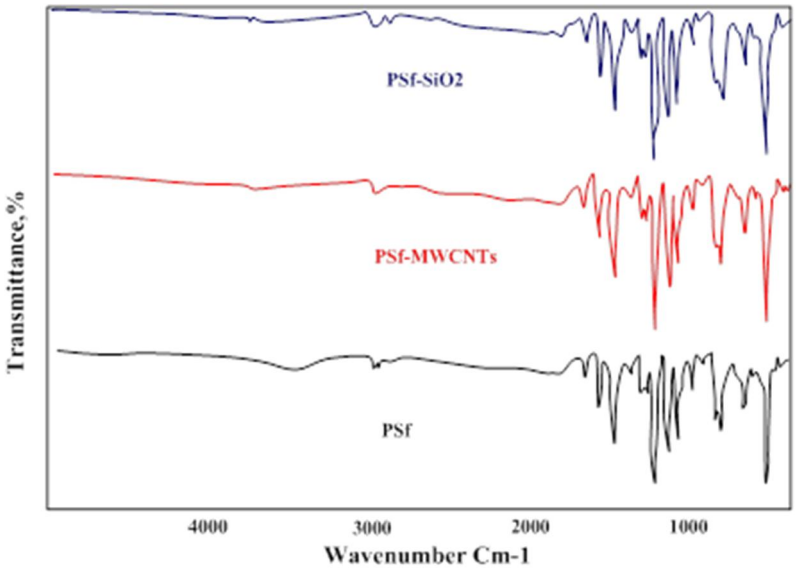

Fig. 10: FTIR of neat and modified Polysulfone membranes.

Membrane performance

This section discussed the effect of different operation condition parameters that may effect on the MD flux of prepared polysulfone membranes (neat and/or modified PSf membranes). This carried out to investigate the optimum condition that gives highest productivity against feed temperature and feed salinity taking into considerations the salt rejection more than 99.9% as follows:

Effect of feed temperature (T_f):

The effect of feed temperature in the range between 40-70 ^oC on neat and modified polysulfone membranes performance was studied. The operation conditions included polymer concentration 15 wt. %, membrane thickness 200±5µm at a constant permeate temperature 10^oC, used distilled water in the permeate tank with TDS 10 ppm and synthetic saline water of NaCl with concentration 5000 ppm in feed tank. Experimental results were plotted in fig. (11).

It was obvious that the increase in feed temperature led to an increase of permeate flux. This effect was attributed to the driving force of mass transfer, which increases with increasing temperature of the feed stream, therefore, the feed temperature has a significant effect on the level of the permeate flux in the MD process (Gryta, 2012).

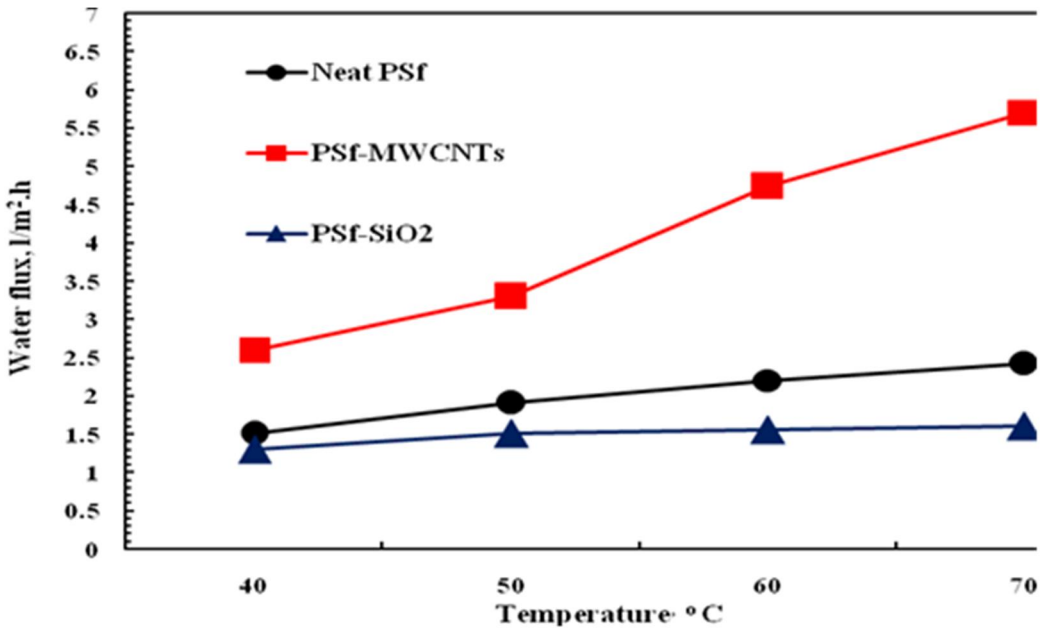

Fig. 11: Effect of feed temperature on neat polysulfone and modified flat sheet membrane.

Effect of feed water concentration

The feed water concentration is a more effective parameter in any desalination process as a value of feed salinity detects what is the desalination technique that could be applied in the desalination process. So, different feed NaCl concentrations synthetic solutions ranged from 5000 to 20000 ppm were used to study the effect of feed concentration on the flux as shown in fig. (12). The operation conditions included PSf membrane of 15 wt.%, and membrane thickness 200 µm at feed temperature 70ºC and the permeate temperature 10ºC.Young, (1947) presented the results of experiments using varying concentrations of sodium chloride and his findings did not differ greatly from those Lee, (1927). Harbeck, (1955) also concluded that the reduction in evaporation is caused by a vapour pressure decrease due to the effects of dissolved solids. Salhorta *et al.* (1985 and 1987); and Oroud, (1994 and 1995) developed models based on computing the effect of salinity on the saturation vapour pressure and incorporated them into Dalton-type formulas to estimate evaporation Figure (12), showed that the increase of the non-volatile solute concentration in the feed aqueous solution led to a reduction of the MD permeate flux. This behavior was attributed to the decrease of the water vapour pressure, the driving force, with the addition of a non-volatile solute in water due to the decrease in water activity in the feed (Khayet and Matsuura, 2011)**.** By another meaning, increasing ionic strength, using NaCl salt, leads to an increase in the boiling point of the solution. This indicates that less water vaporization can occur at the membrane surface, which diminishes the amount of vapour transported through the membrane pores (Gazagnes *et al.,* 2007)**.** Also, while the ionic strength of the feed solution increases, the dynamic fluid will change as a result of increasing viscosity and then the concentration polarization should be added to the temperature polarization, which reduces the imposed DCMD driving force and then the permeate flux (Schofield *et al.,* 1990) .

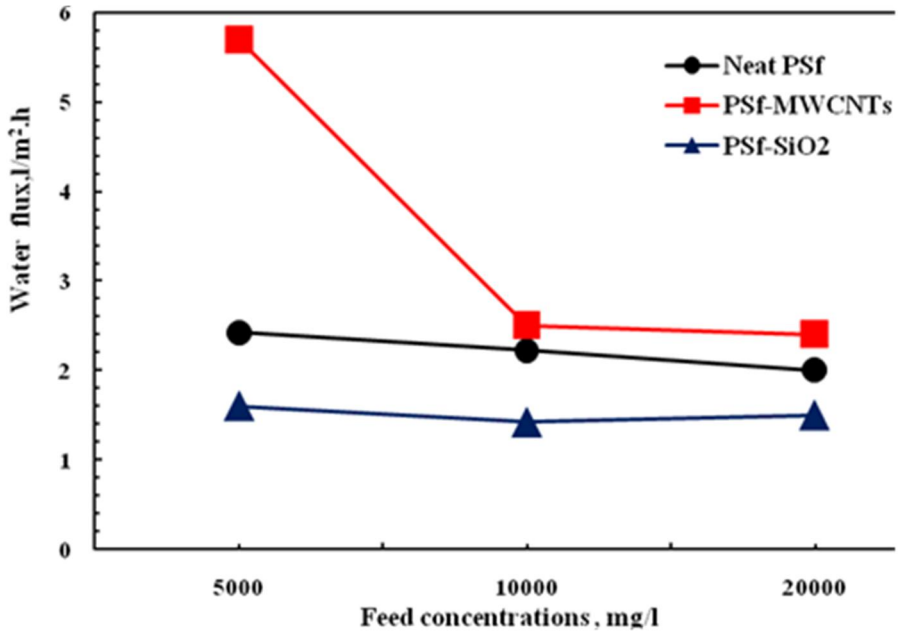

Fig. 12. Effect of feed water concentration on neat polysulfone and modified flat sheet membrane.

Application

Hydrochemical species

Due to desalination process of five thermal groundwater in coastal east area at Gulf of Suez, the hydrochemical species is changed as to pH increased in all reject water samples than feed water after desalination Fig. (13. A). This increased related to change of HCO_3^-salt to CO_3^{--} salt in water.

Figure (13. B, C, D, E, F, G, H, & I) for TDS , Na^+, Ca^{++}, Mg^{++},K^+,HCO_3^{--}, SO_4^{--},and Cl^-) showed, the concentration of these ions in five thermal groundwater are increased due to water extract by this desalination process. Moreover for K^+ and SO_4^{--}concentration are fluctuated between increase and decrease for feed and reject after desalinating process. But in all samples the HCO_3^- concentration was decreased after desalination process due to change of bicarbonate salt to carbonate forms by increased the temperate as to equations:

$$2HCO_3^- \longrightarrow CO_3^{--}+CO_2+H_2O$$

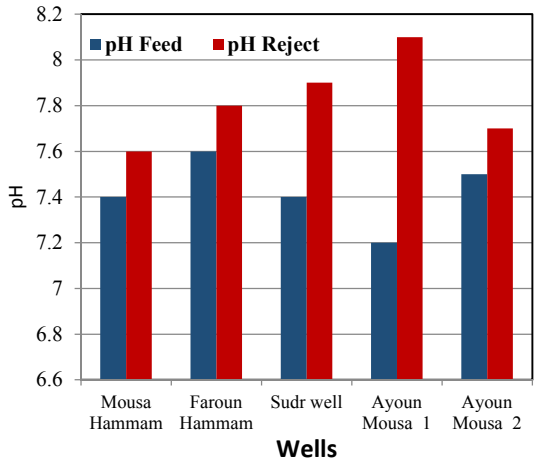
pH Feed
pH Reject
pH
8.2
8
7.8
7.6
7.4
7.2
7
6.8
6.6
Mousa Hammam
Faroun Hammam
Sudr well
Ayoun Mousa 1
Ayoun Mousa 2
Wells

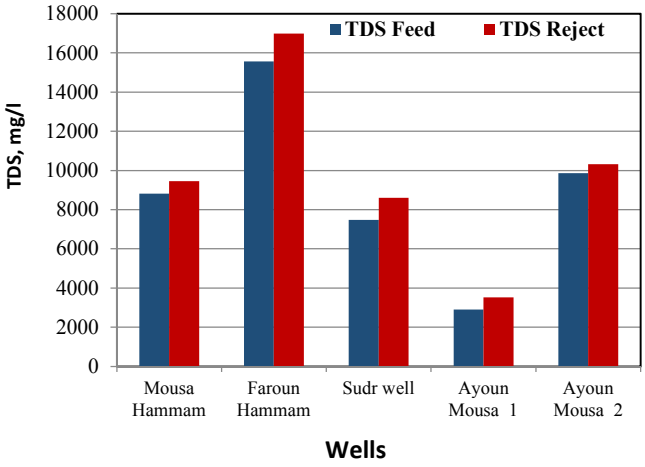
TDS Feed
TDS Reject
TDS, mg/l
18000
16000
14000
12000
10000
8000
6000
4000
2000
0
Mousa Hammam
Faroun Hammam
Sudr well
Ayoun Mousa 1
Ayoun Mousa 2
Wells

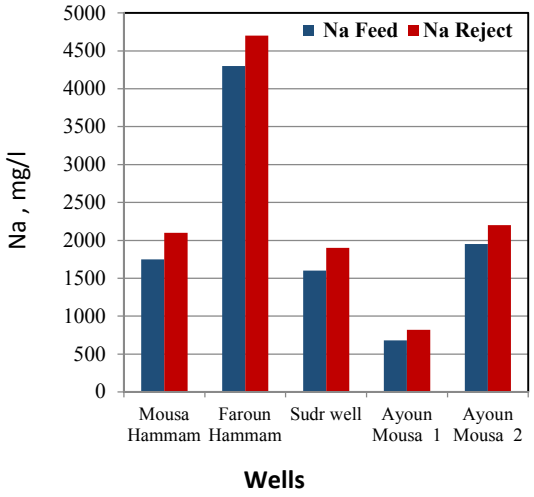
Na Feed
Na Reject
Na , mg/l
5000
4500
4000
3500
3000
2500
2000
1500
1000
500
0
Mousa Hammam
Faroun Hammam
Sudr well
Ayoun Mousa 1
Ayoun Mousa 2
Wells

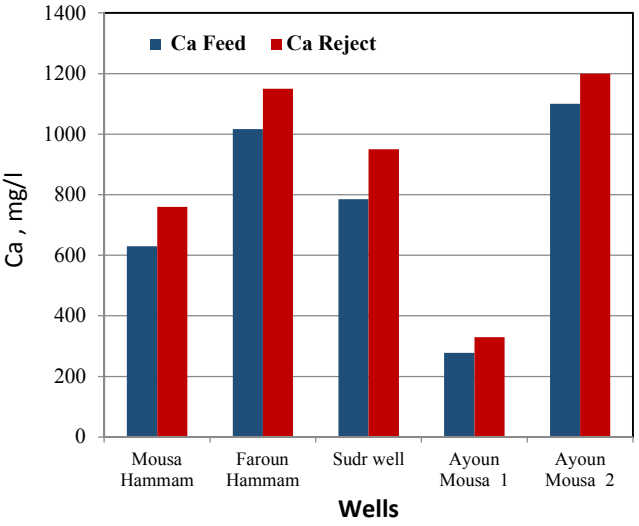
Ca Feed
Ca Reject
Ca , mg/l
1400
1200
1000
800
600
400
200
0
Mousa Hammam
Faroun Hammam
Sudr well
Ayoun Mousa 1
Ayoun Mousa 2
Wells

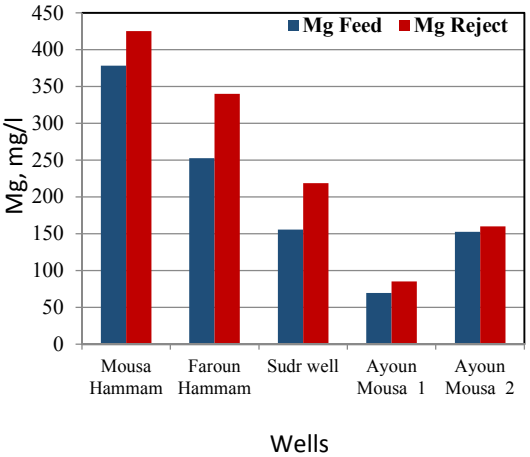
Mg Feed
Mg Reject
Mg, mg/l
450
400
350
300
250
200
150
100
50
0
Mousa Hammam
Faroun Hammam
Sudr well
Ayoun Mousa 1
Ayoun Mousa 2
Wells

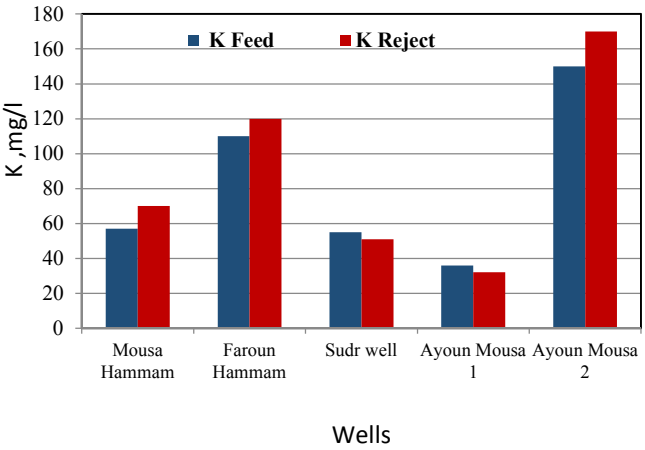
K Feed
K Reject
K ,mg/l
180
160
140
120
100
80
60
40
20
0
Mousa Hammam
Faroun Hammam
Sudr well
Ayoun Mousa 1
Ayoun Mousa 2
Wells

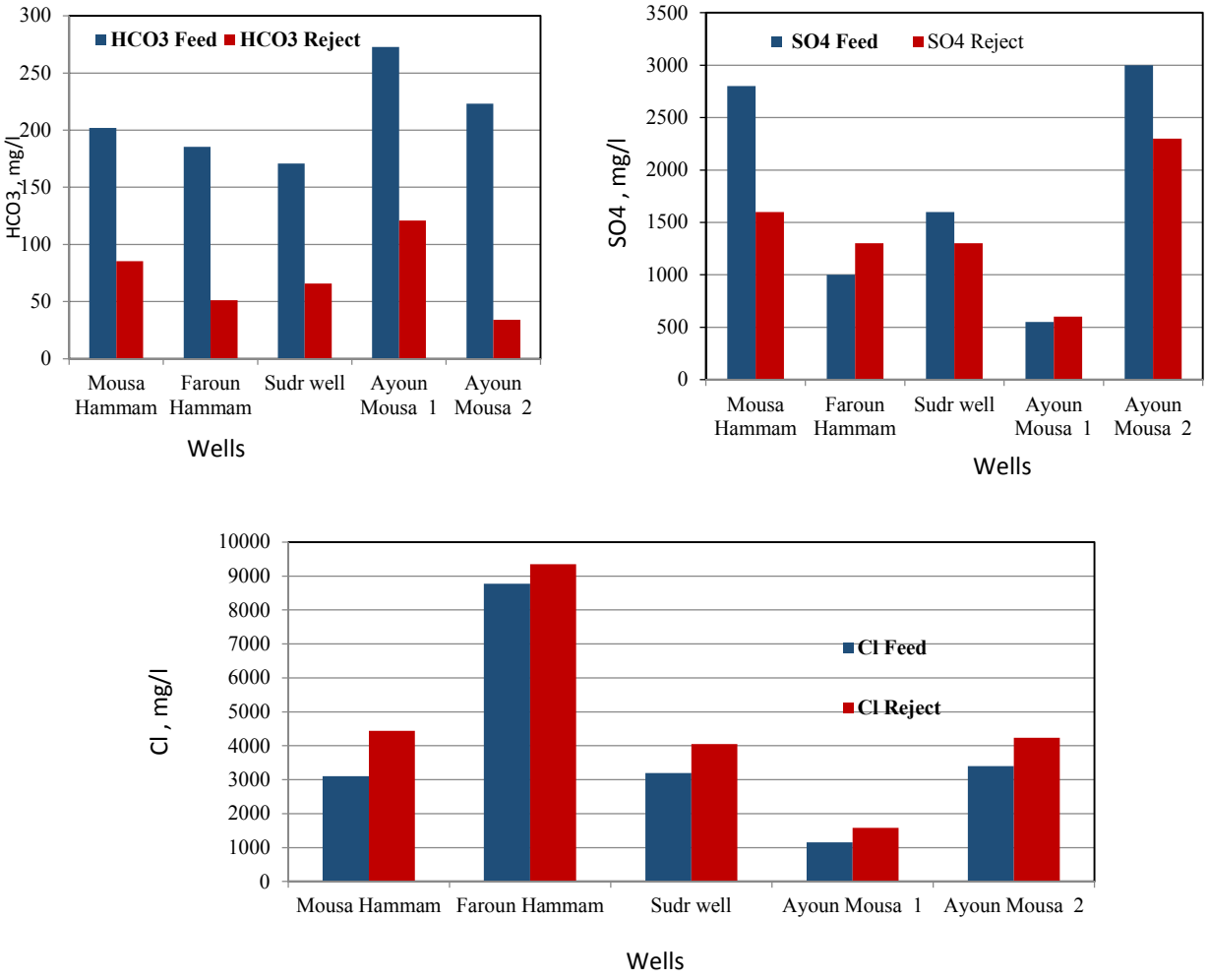

Fig. 13: Hydrochemical species of major cations and anions before and after desalination process in five thermal groundwater at the study area

Performance of neat and modified polysulfone membranes

Five thermal groundwater samples were collected from the study area and applied as feed water in membrane distillation unit to be desalinated using the three membranes (PSf, PSf/SiO_2, PSf/CNT). The chemical analyses were done for these samples before and after desalination as shown in table (1). The membranes flux were shown in figs. (14 & 15) and operation conditions in table (3).

PSf/CNT nano-composite membrane showed the best flux when compared to that of neat PSf membrane and PSf/SiO_2.

Effect of feed water salinity

Figure (14) at 40 °C of feed temperature and 10 °C permeate temperature with feed flow and permeate flow 1L/min. Three thermal groundwater have different salinity (2900, 8818, and 10316 ppm) were tested to measure the performance of desalination process by MD technique on three synthesized membranes.

From fig.(14), we fund that when PSf/CNT membrane used for water desalination the flux was 1.76 L/m^2.h, more than 1.1 and 1.5 L/m^2.h of PSf/ SiO_2 and PSf membranes for salinity 2900 ppm of Ayoun Mousa 1 thermal groundwater. But in high salinity at 40°C for PSf/CNT membrane the water

flux decreased from 1.76 to 1.65 and 1.45 L/m^{2}h. Also, water flux of PSf/SiO_2 and neat PSf decreased from 1.1, 0.99, 0.99 and 1.5, 1.43 and 1.32 L/m^{2}h, respectively.

Figure (15) at 70 °C of feed flow and 10 °C of permeate flow with feed flow and permeate flow 1L/min. Two thermal groundwater had different salinity (7482 and 15574 ppm) were tested to measure the performance of desalination process by MD technique on three synthesized membranes.

From fig. (15), we found that when neat PSf/CNT membrane used for water desalination the flux was 1.37 L/m^{2}h, more than 0.55 and 1.2 L/m^{2}h of PSf/ SiO_2 and PSf membranes for salinity 7482 ppm of Sudr well thermal groundwater. But in high salinity at 70°C for PSf/CNT membrane the water flux decreased from 1.37 to 1.2. L/m^{2}h. Also, water flux of neat PSF decreased from 1.2 to 1.1 L/m^{2}h.

The second law of thermodynamics implies that an increase in ion activity because of the presence of solute reduces the chemical potential of a liquid solvent and the rate of spontaneous transformation of a liquid phase into a vapour phase (Oroud, 1999 and Sandler, 1989) [33, 34]. This arises from the additional disorder imposed on the solvent that retards the transformation of the solution into the vapour phase, which is a somewhat more disorderly phase (Atkins, 1994).

Effect of feed water temperature

At 40°C of three thermal groundwater (Ayoun Mousa 1, 2 and Hamamm Mousa) the maximum flux achieved (1.78 L/m^2 h) for PSf/CNT nano-composite membrane when compared with (1.1 and 1.5 L/m^2 h) for neat PSf/SiO_2 and PSf membranes respectively. But at 70°C of two thermal groundwater (Hamamm Foroun and Sudr well) the maximum flux was achieved 1.37 L/m^2 h for PSf/CNT nano- composite membrane to 0.55 and 1.2 L/m^2 h of PSf /SiO_2 and neat PSf, respectively. It is known that the increase in temperature of salt water in comparison with fresh water (Sanchez, 1995) is another result of the increase in ion activity coefficient that depends on salt concentration.

It is obvious that the MWCNTs enhanced the performance of MD technique than SiO_2 when added to PSf membrane with the same operating conditions (Roy *et al.,* 2014). The results also show that the increase in feed salinity results in a reduction of the MD permeate flux. This behavior is attributed to the decrease in the water vapor pressure, the driving force, with the addition of non-volatile solute in water due to the decrease in water activity in the feed (Hwang *et al.,* 2011 and Winter *et al.,* 2012).

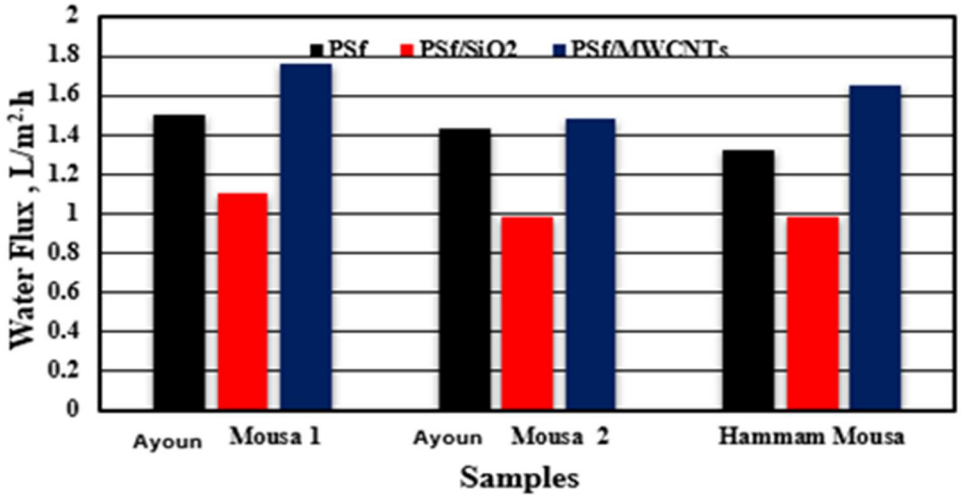

Fig. 14: Permeate flux of three different samples using different membranes.
Flow rate of hot water = 1 L/min., flow rate of cold water = 1 L/min., Temperature of hot feed = 40 ° C, temperature of cold water = 10 ° C.

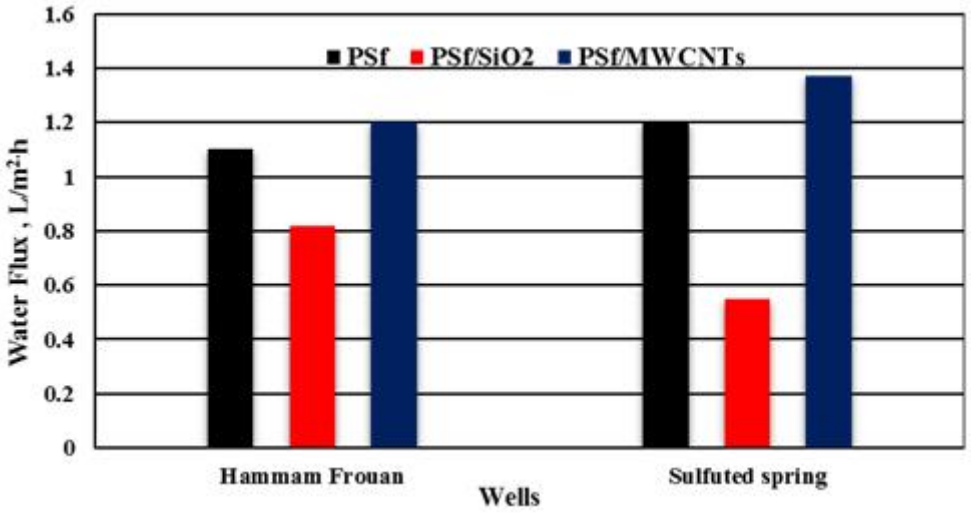

Fig. 15: Permeate flux of two different samples using different membranes.
Flow rate of hot water = 1 L/min., flow rate of cold water = 1 L/min., Temperature of hot feed = 70 ° C temperature of cold water = 10 ° C.

Table 3: Permeate flux of five thermal groundwater samples by different membranes at different temperature 40 and 70 ° C.

Permeate flux L/m².h	Ayoun Mousa 1	Ayoun Mousa 2	Hammam Mousa	Hammam Frouan	Sudr well
PSf	1.5	1.43	1.32	1.1	1.2
PSf/SiO_2	1.1	0.99	0.99	0.82	0.55
PSf/CNTs	1.76	1.48	1.65	1.2	1.37
F hot= 1 L/min. F cold= 1 L/min.				**F hot= 1 L/min. F cold= 1 L/min.**	
T hot = 40 °C T cold= 10 °C				**T hot = 70 °C. T cold= 10 °C**	

Conclusion

The most important areas of geothermal manifestation are located along the Gulf of Suez coastal zones. Hot springs in these areas include Hammam Faroun, which contains thermal water reaching the highest temperature ranged from70 °C) and salinity 15574 mg/l, as well as Ayoun Mousa 1, 2, Hammam Mousa and Sudr well. The hot spring sites are located in topographically low areas, covered with wadi deposits, and surrounded by fractured Eocene limestone. They are characterized by high-order drainage patterns and flow toward the Gulf of Suez coastal zones.

The value of the estimated potential for electric generation was 19.8 MW. This value would be enough for the desalination of water for human and agricultural consumption and can thereby be used for sustainable development in Sinai Peninsula.

Direct contact membrane distillation was used to desalinate thermal water in these areas. The polysulfone membrane modified with multi-walled carbon nanotubes gave the best result in permeate flux 1.76 and 1.37 l/m².h at (40 and 70°C) feed temperature and feed salinity 2900 to 15574 mg/l compared to neat PSf and PSf/ SiO_2 membranes which give water flux 1.5 to 1.1 and 1.1 to 0.99 l/m².h at feed temperature (40 and 70°C) and 7482 to 9864 mg/l feed salinity.

Recommendations

From previous study, the results of desalination process carried by membrane distillation, the samples were collected after from the springs at site then analysis in laboratory of the Desert Research Center, which is located far about 250 to 450 km. This reduces the utilization of high temperature. Therefore, it is preferable to have two desalination works in site to take advantage of the

high temperature, which ranges from 40 ° C to 70 ° C in one of the methods of desalination, which depends on the membrane, including membrane distillation (MD) or Reverse Osmosis (RO).

First: Membrane distillation process: in this process need to high temperature to use as a source to heat the recharge water to reach 40 or 70 ° C from 25 ° C or lower than. So this heat obtains from the hot thermal springs which reduced the capital cast of production one meter cube potable water from saline water to sustainable development of these areas.

Second: Reverse Osmosis process: The high temperature of the hot thermal water springs maximum 45 °C reduced a feed pressure than 25 °C. Thus reduces the Specific energy consumption (SEC) used for desalination of saline or brackish water, fig (16). Mean while the cost of desalination by this method reduced.

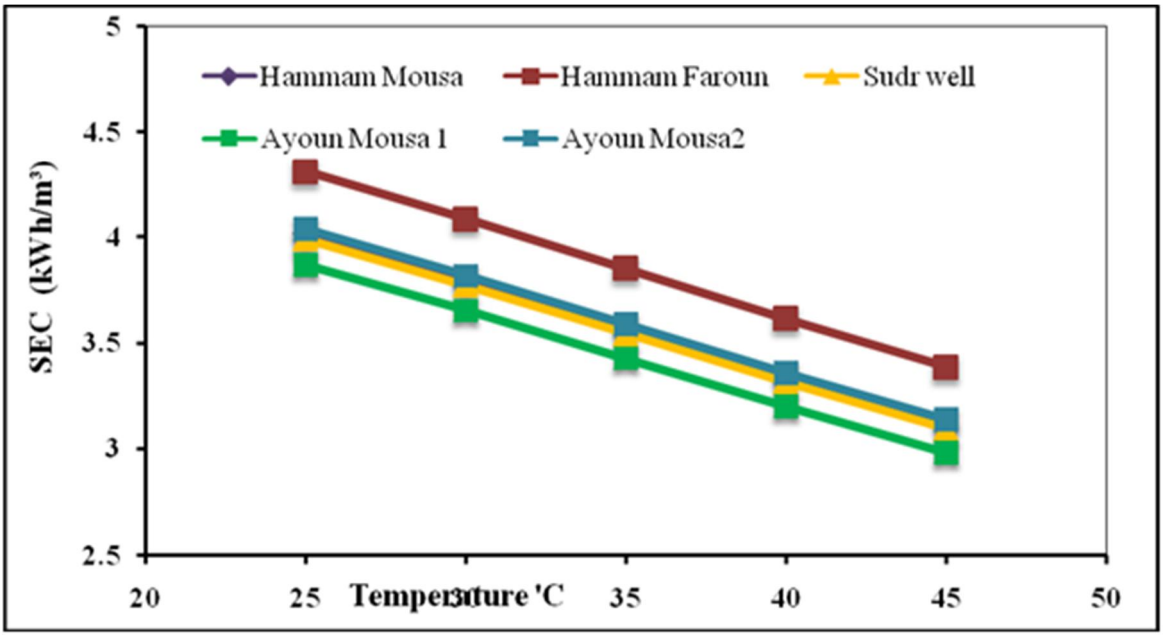

Fig. 16: Specific energy consumption Vs temperature of hot springs wells in coastal area in Gulf of Suez.

Acknowledgement

The authors acknowledge financial support for this work from the Science and Technological Development Fund (STDF) in Egypt through Grant 5240 (Egyptian Desalination Research Center of Excellence, EDRC.

References

Abdel Zaher, M., J. Nishijima, Y. Fujimitsu and S. Ehara, 2011. Assessment of low-temperature geothermal resource of Hammam Faraun hot spring, Sinai Peninsula, Egypt. In: Proceedings, 36 Workshops on Geothermal Reservoir Engineering. Stanford, California: Stanford University, SGP-TR-191.

Arsalan, K., A. A. Abdulhadi, C.A. Othman, L. Tahar and K. M. A. Zafarullah, 2015. Preparation and properties of nano-composite polysulfone/multi-walled carbon nanotubes membranes for desalination" Desalination, 367:134–144 .

Atkins, P.W., 1994. The Second Law. Scientific American Books: New York.

Chakrabarty, B., A.K. Ghoshal and M.K. Purkait, 2008. Effect of molecular weight of PEG on membrane morphology and transport properties. J. Membr. Sci. 309, 209–221.

El Fiky A., 2009. Hydrogeochemistry and geothermometry of thermal groundwater from theGulf of Suez region, Egypt. Earth Science, (2):71e96;

El Ramly, I.M., 1969. Recent review of investigations on the thermal and mineral springs in the U. A. R. Proceedings of the XXIII International Geological Congress 19: 201-213.

Gazagnes L., S. Cerneaux, M. Persin, E. Prouzet and A. Larbot, 2007. Desalination of sodium chloride solutions and seawater with hydrophobic ceramic membranes. Desalination 217 ; 260–266.

Gryta, M., 2012. Effectiveness of Water Desalination by Membrane Distillation Process. Membranes, 2, 415-429.

Harbeck, G.E., 1955. The effect of salinity on evaporation. United States, Geological Survey, Professional Papers 272-A.

Hwang, H.J., K. He, S. Gray, J. Zhang and I.S. Moon, 2011. Direct contact membrane distillation (DCMD): Experimental study on the commercial PTFE membrane and modeling, Journal of Membrane Science 371:pp.90–98.

Jonsson, A. S., R. Wimmerstedt and A. C. Harrysson, 1985. Membrane distillation - A theoretical study of evap. through microporous membranes. Desalination, vol. 56, pp. 237-249.

Khare, V. P., A. R.Greenberg, J. Zartman, W.B. Krantz and P. Todd, 2002. "Macrovoid pore formation in dry-cast cellulose acetate membranes: buoyancy studies. J. Membr. Sci.205 (1) 11-21.

Khayet, M. and T. Matsuura, 2011. Membrane distillation principles and applications. Elservier B.V., ch. 10, pp. 254-268.

Lashin A., 2007. Evaluation of the geothermal potential around the coastal parts of theGulf of Suez-Egypt, using well logging and geothermometer data. Journal of Applied Geophysics 2007; 6(2):215e48.

Lee, C.H., 1927. Discussion of 'Evaporation on reclamation projects' by I.E. Houk. Transactions of the American Society of Civil Engineers 90:340–343.

Madaeni, S., S .Zinadini and V. Vatanpour, 2013. Preparation of super hydrophobic nano-filtration membrane by embedding multi-walled carbon nanotube and polydimethylsiloxane in pores of microfiltration membrane", Sep. Purif. Technol. 111 (2013) 98–107.

Nicholson, K. (1993) Geothermal Fluids; Chemistry and Exploration Techniques, Springer, Berlin.

Okiel, K., A. M. El-Aassar, T. Temraz, S. El-Etriby and H.A. Shawky (2015): Performance assessment of synthesized CNT/ polypropylene composite membrane distillation for oil field produced water desalination, Desalination and Water Treatment, DOI: 10.1080/ 19443994. 1044475

Oroud, I.M. 1994. Evaluation of saturation vapor pressure over hyper saline solutions at the southern edge of the Dead Sea, Jordan. Solar Energy53: 497–503.

Oroud, I.M., 1995. Effects of salinity upon evaporation from pans and shallow lakes near the Dead Sea. Journal of Theoretical and Applied Climatology 52: 231–240.

Oroud, I.M., 1999. Temperature and evaporation dynamics of saline solutions. Journal of Hydrology 226: 1–10.

Pipers, A.M., (1953). A graphic procedure in the geochemical interpretation of water analysis. Amer. Geoph. Union Trans. 25 (105), 914- 923.

Pourya, M., A.I. Nor, M.Z.W. Wan and A.Y. Nor, 2015. Study of Morphology and Gas Separation Properties of Polysulfone/Titanium Dioxide Mixed Matrix Membranes. Polymer Engineering and Science.

Priya, D., P. Sivakumar and M .Sutha (2014) "A Review on Desalination using Membrane Distillation: Status and Potential" Int. J .Chem Tech Res., 6(9), pp 4259-4263.

Roy, S., M. Bhadra and S. Mitra, 2014. Enhanced desalination via functionalized carbon nanotube immobilized membrane in direct contact membrane distillation, Separation and Purification Technology, 136:pp.58–65.

Said, M.M., A.M. El-Aassar, Y.H. Kotp, H.A. Shawky, and M.S.A. Abdel Mottaleb, 2013. Performance assessment of prepared polyamide thin film composite membrane for desalination of saline groundwater at Mersa Alam-Ras Banas, Red Sea Coast, Egypt. Desalination water treat. 51(1-3), 1-11.

Salhorta, A.M., E.E. Adams and D.R.F. Harleman, 1987. The alpha, beta, gamma of evaporation from saline water bodies. Water Resources Research 23:1769–1774.

Salhotra, A.M., E.E. Adams and D.R.F. Harleman. 1985. Effects of salinity andionic composition on evaporation: analysis of Dead Sea evaporationpans. WaterResources Research 21: 1336–1344.

Salim, M.G., Selection of groundwater sites in Egypt, using geographic information systems, for desalination by solar energy in order to reduce greenhouse gases, J. Adv. Res. 3 (2012) 11–19.

Sanchez, J.M., 1995. Order–disorder transitions. In Encyclopedia of Applied Physics, vol. 13, Trigg GL (ed.). VCH: New York: 1–16.

Sandler, S.I. 1989. Chemical and Engineering Thermodynamics. Wiley: New York

Schoeller, H., 1962. Geochmie des eaux Souteraines. Rev. De l'Institue Français du Petrole, 10, 230-244.

Schofield, R. W., A. G. Fane and C. J. D. Fell, 1990. Factors affecting flux in membrane distillation. Desalination , Vol. 77, pp. 279–294.

Shata, A.A. (1990) Thermal springs and mineralized water in the Gulf of Suez taphrogenic basin, northeast Egypt, Memoires of the 22nd Congress of IAH, XXII, Lausanne: 681-688.

Sturchio, N.C., G.B. Arehart, M. Sultan, Y. Sano, Y. Abo Kamar and M. Sayed, 1996. Composition and origin of thermal waters in theGulf of Suez area, Egypt. Applied Geochemistry, 1(1):471e9.

Sturchio, N.C., G.B.Arehart, M. Sultan, Y. Sano, Y. Abo Kamar and M. Sayed, 1996. Composition and origin of thermal waters in the Gulf of Suez area, Egypt, Applied Geochemistry, 11: 471-479.

Winter, D., J. Koschikowski and S. Ripperger, 2012. Desalination using membrane distillation: Flux enhancement by feed water deaeration on spiral-wound modules, Journal of Membrane Science, 423–424:pp.215–224.

Young, A. A. 1947. Some recent evaporation investigations. Transactions, American Geophysical Union 28: 279–284.

Yuxin, M., S. Fengmei, M. Jun, W.Miaonan, Z. Jun, and G.Congjie, 2011. Effect of PEG additive on the morphology and performance of polysulfone ultrafiltration membranes. Desalination 272, 51-58.